

## New method for rock qualification Új módszer az építőkövek minősítésére

Lőrincz János<sup>1</sup>, Imre Emőke<sup>2</sup>; Trang Phong. Q<sup>1</sup>.  
IBME, 2Óbudai Egyetem, imre.emoke@kvk.uni-obuda.hu tqp0322@gmail.com

Gálos Miklós, Kárpáti László  
Szilikátipari Tudományos Egyesület Kő és Kavics Szakosztály miklos.galos@gmail.com [karpati@szte.org.hu](mailto:karpati@szte.org.hu)

Talata István  
SZIE Ybl Miklós Faculty of Architecture and Civil Engineering, Budapest [talata.istvan@ybl.szie.hu](mailto:talata.istvan@ybl.szie.hu)

Daniel Barreto  
Edinburgh Napier University, U.K. [d.barreto@napier.ac.uk](mailto:d.barreto@napier.ac.uk)

Francesca Casini<sup>3</sup>, Giulia Guida<sup>4</sup>  
<sup>3</sup>Università di Roma Tor Vergata [francesca.casini@uniroma2.it](mailto:francesca.casini@uniroma2.it),  
<sup>4</sup>Università Niccolò Cusano [giulia.guida@unicusano.it](mailto:giulia.guida@unicusano.it)

**ÖSSZEFOGLALÁS:** A kutatás során egy mozsaras törési kísérlet került kialakításra, amellyel a kőzetek törési sebessége a szemeloszlási entrópia segítségével minősíthető. A szemeloszlás-változás pályája az entrópia diagramban a különböző homokok esetén azonos volt, csak a sebesség tért el. A törés sebességét egy entrópia koordináta, az átlagos logaritmikus szemcseméret adott terhelésre eső változásának mérőszáma adhatja meg. A kutatás mellék-termékeként az is kimutatható volt, hogy a belső stabilitás és a törési/degradációs folyamat kapcsolatban áll egymással. Ha a törés kezdetén megjelenik néhány kisebb frakció, a normalizált entrópia pályán felépő szakadás révén a pálya kikerül az entrópia diagram instabil részéről. Ezt követően a pálya eléri a normalizált entrópia diagram felső határvonalát, majd ezen halad, ahol minden szemeloszlás fraktál. Az entrópia elv alapján magyarázható, hogy a természetben található szemeloszlások fraktál dimenziója általában 3-nál kisebb.

kulcsszavak: kőzetminősítés, törés, fraktál eloszlás, belső stabilitás

**ABSTRACT:** A new method was elaborated to characterize the breakage properties of rocks. A crushing test was suggested and parallel tests were performed on sand-pairs with different parent rocks, using identical initial gradings. The data were analysed using the grading entropy theory, the grading curve variation was represented in the entropy diagram (with a coordinate uniquely related to the mean log diameter). The results with various rocks with the same conditions indicated the same entropy path, only the speed was different. Based on this, a new testing method can be suggested. As a by-product of the result, it is shown that the breakage path and the internal stability of soils seem to be linked. The discontinuity of the normalised entropy path at the appearance of some finer fractions drifts out the normalised entropy path from the unstable part of the diagram. A second consequence is the explanation why fractal distribution with fractal dimension  $n < 3$  is so frequent in nature.

keywords: rock qualification, breakage, fractal distribution, internal stability

## 1 INTRODUCTION

### 1.1 Fragmentation in nature

The fragmentation phenomena in nature are described by a power law distribution. The size distribution of fragments:

$$N(\Delta \leq d) \sim d^{-n} \quad (1)$$

where  $N$  is the number of particles that have diameters  $\Delta$  below the size  $d$ .

The fractal distribution law is independent of the material properties, the energy input and the relevant length scales. Value of negative exponent is called as 'fractal dimension' and is between 2 to 3 for 3

dimensional objects (Kun (2017)). Fractal distributions are naturally occurring in granular materials, such as meteorites, gouge material, avalanches, mines and in laboratory tests, like compression tests and shear tests (Hartmann (1969), Bridgwater et al (2013), Sammis et al (1987), Airey and Kelly (2008), Imre et al (2010)). In space mechanics, fractal dimension  $\sim 3$  is encountered for small particles at the planetary rings,  $\sim 6$  for large ones with size  $\sim 0.1-1$  km (Brillantov (2015)). The monotonic laboratory tests present a range of fractal dimension, between 2.20 and 2.91 (McDowell et al (1996), Luzzani and Coop (2002), Palmer and Sanderson (1991), Steacy and Sammis (1991), Roberts and de Souza (1958), Hagerty et al (1991), Pál et al (2016), Coop et al (2004)).

## 1.2 Aim of the paper

The aim of the research is to study the breakage and degradation process and, to elaborate a new method to characterize the rock material properties in terms of degradation or fragmentation. For this aim, a crushing test is combined with the grading entropy theory to describe the path and the rate of breakage in terms of grading curve.

In this paper at first the grading entropy theory, the concept of the entropy coordinates, the optimal or fractal grading curves, the (discontinuity of the) breakage path and the grading entropy based internal stability criterion are presented. Then the result of some breakage tests elaborated in this research are presented in the entropy diagram. In addition, the entropy path of a degradation (open pit mine) case study and, some tests entailing breakage, performed all in relation to this research are reanalysed.

It is found, that the path may contain an initial discontinuity, a linear part and, a curved part where all distributions are fractal with increasing fractal dimensions until 3. Similar paths and fractal dimensions occur in the nature as in the laboratory tests. The breakage path is independent of the rock material, its rate is dependent on the material only. The linear part of path being completed by a theoretically computed starting point is proved to be one possible way for breakage rate characterization.

## 2 GRADING ENTROPY

### 2.1 The space of the grading curves

The grading curve is the distribution of the log diameter of the grains  $d$  by dry weight. In the grading curve measurement the sieve hole diameters, and as a result, the fraction limits are doubled. An abstract fraction system is defined as follows. The diameter range for fraction  $j$  ( $j = 1, 2, \dots, j$  see Table 1, Lőrincz (1986)) are defined by using the integer powers of the number 2 (Imre et al., 2009).

$$2^j d_0 \geq d > 2^{j-1} d_0, \quad (2)$$

where  $d_0$  is the smallest diameter which may be equal to the height of the SiO<sub>4</sub> tetrahedron ( $2^{-22}$  mm). The 2 base log of the diameter limits are integers, called abstract diameters. The relative frequencies of the fractions  $x_i$  ( $i = 1, 2, 3, \dots, N$ ) for each grading curve fulfil the following equation:

$$\sum_{i=1}^N x_i = 1, \quad x_i \geq 0, \quad N \geq 1 \quad (3)$$

where the integer variable  $N$  – the number of the fractions between the finest and coarsest non-zero fractions – is used. The relative frequencies  $x_i$  can be identified with the barycentre coordinates of the points of an  $N-1$  dimensional, closed simplex (which is the  $N-1$  dimensional analogy of the triangle or tetrahedron, the 2 and 3 dimensional instances) and, the space of the grading curves with  $N$  fractions can be identified with the  $N-1$  dimensional, closed simplex. The vertices of the simplex represent the fractions, and the 2 dimensional edges are related to the two-mixtures etc. The sub-simplexes of a simplex are partly continuous, and partly gap-graded. The continuous sub-simplexes have a lattice structure, as is indicated in Fig 1.

**Table 1.** Definition of fractions. (A  $j$ -dik frakció definíciója és saját entrópiája)

$j$	1			...	23	24
Limits	$d_0$ to $2 d_0$			...	$2^{22} d_0$ to $2^{23} d_0$	$2^{23} d_0$ to $2^{24} d_0$
$S_{0j}$ [-]	1			...	23	24

### 2.2 Entropy parameters

The grading entropy  $S$  is a statistical entropy, modified for the unequal cells (fractions are doubled, Lőrincz (1986)). It can be separated into the sum of two parts. The grading entropy  $S$ :

$$S = S_0 + \Delta S \tag{4}$$

where  $S_0$  is called the base entropy and  $\Delta S$  the entropy increment. The base entropy:

$$S_0 = \sum x_i S_{0i} = \sum x_i i \tag{5}$$

where  $S_{0i}$  is the grading entropy of the  $i$ -th fraction, being identical to the fraction serial number (Table 1). The normalized or relative base entropy  $A$ :

$$A = \frac{S_0 - S_{0\min}}{S_{0\max} - S_{0\min}} \tag{6}$$

where  $S_{0\max}$  and  $S_{0\min}$  are the entropies of the largest and the smallest fractions, respectively. The entropy increment  $\Delta S$  is:

$$\Delta S = -\frac{1}{\ln 2} \sum_{x_i \neq 0} x_i \ln x_i. \tag{7}$$

which varies between 0 and  $\ln N / \ln 2$ , depending on the fraction number  $N$ . The normalized entropy increment  $B$ :

$$B = \frac{\Delta S}{\ln N} \tag{8}$$

### 2.3 Entropy diagrams, optimal grading curves, and inverse image

Any grading curve can be represented as a single point in terms of the entropy coordinates. Four maps can be defined between the  $N-1$  dimensional, open simplex (fixed  $N$ ) and the two dimensional real Euclidean space of the entropy coordinates, the non-normalized  $\Delta \rightarrow [S_0, \Delta S]$ , normalized  $\Delta \rightarrow [A, B]$ , partly normalized  $\Delta \rightarrow [A, \Delta S]$  or  $[S_0, B]$ .

The images – the entropy diagrams – are compact, like the simplex (Figs 1, 2) . The inverse image of the regular values is similar to an  $N-3$  dimensional sphere, “centered” to the optimal point (Fig 2). The inverse image of the maximum normalized entropy increment lines  $B$  is the optimal line (Fig 2). The value of  $d_{\min}$  is indifferent for the normalized diagram, eg., all fractions map into  $A = 1$ .

The optimal grading curve or simplex point with maximal  $B$  for a specified  $A$  is as follows. The entropy increment  $B$  is strictly concave function, with a unique conditional maximum point for each  $A = \text{const}$  value. This single optimal point or unique optimal grading curve is defined as follows: The following - so-called optimal - grading curve or point of the simplex maps at fixed  $A$  on the maximum  $B$ :

$$x_1 = \frac{1}{\sum_{j=1}^N a^{j-1}} = \frac{1-a}{1-a^N}, \quad x_j = x_1 a^{j-1} \tag{9}$$

where parameter  $a$  is the root of the following equation :

$$y = \sum_{j=1}^N a^{j-1} [j-1 - A(N-1)] = 0. \tag{10}$$

The single positive root  $a$  varies continuously between 0 and  $\infty$  as  $A$  varies between 0 and 1,  $a=1$  at the symmetry point ( $A=0.5$ ) and  $a>1$  on the  $A>0.5$  side of the diagram [19]. The equation of finite fractal distribution (Einav 2007):

$$F(d) = \frac{d^{(3-n)} - d_{\min}^{(3-n)}}{d_{\max}^{(3-n)} - d_{\min}^{(3-n)}} \tag{11}$$

where  $d$  is particle diameter,  $n$  is fractal dimension. Taking into account that in the grading entropy theory the fraction limits are defined by using the integer powers of the number 2, it can be derived that the relative frequencies of the fractions  $x_i$  ( $i = 1, 2, 3...N$ ) are as follows:

$$x_j = x_1 a^{j-1} \quad \text{where} \quad x_1 = \frac{(2^{(3-n)} - 1) d_{\min}^{(3-n)}}{d_{\max}^{(3-n)} - d_{\min}^{(3-n)}}, \quad a = 2^{(3-n)} \quad \text{or} \quad n = 3 - \frac{\log a}{\log 2} \tag{12}$$

It follows that the optimal grading curves have finite fractal distribution, the fractal dimension  $n$  varies between 3 and  $-\infty$  on the  $A > 0.5$  side as  $a$  varies between 1 and  $\infty$ ,  $n$  varies between 3 and  $-\infty$  on the  $A < 0.5$  side of the maximum normalized entropy increment line, as  $a$  varies between 1 and 0. The  $n$  depends on  $N$  except at the symmetry point of the diagram ( $A = 0.5, B = 1/\ln 2, n = 3, a = 1$ ). The global maximum of the grading entropy  $S$  is related to such an optimal point where  $n = 2, a = 2$  (Table 2, Fig 3). The optimal grading curve is concave if  $A < 0.5$ , linear if  $A = 0.5$ , convex if  $A > 0.5$  (Fig 4).

### 2.4 Stability criterion and stable fractal dimensions

Some domains and points of the entropy diagrams were successfully related to internal or grain structure stability on the basis of vertical water flow tests Lőrincz (1986). On the basis of the suffosion test results, the three basic types of soil structures were related to three domains of the normalized entropy diagram (Fig 5). In Zone I ( $A < 2/3$ ) no structure of the large grains is present, the coarse particles “float” in the matrix of the fines and become destabilized when the fines are removed by piping. The physical content of criterion is that parameter  $A$  expresses the proportion of the large grains, which form structure if they are present in large enough quantity. In the zone II, the coarse particles start to form a stable skeleton and total erosion cannot occur. In Zone III, the structure of larger particles is inherently stable. The division curve between II and III connects the maximum entropy points with fraction number less than  $N$  (Figs 3, 5).

Although the fractal dimension  $n$  may vary from minus to plus infinity as the relative base entropy  $A$  (normalized mean log scale diameter) varies between 0 and 1, in the function of  $N$ , only a few of them are stable. The fractal distribution is unstable in terms of grading entropy criterion if  $A$  is less than  $A = 0.66$ . The related  $n$  depends on  $N$ , it is 2,62 for  $N = 7$ , it is 2,25 for  $N = 3$ , it is 2.96 for  $N = 30$ . The fractal distribution is stable if  $n < 2$  (independly of  $N, A$ ). The transitional stability zone is situated between the fractal dimension of to  $A = 0.66$  varying in the function of  $N$ , and fractal dimension  $n = 2$ .

### 2.5 Discontinuity of the path

Let us assume that the grading curve “continuously” varies due to breakage. If  $N$  varies, the non-normalized entropy path of the grading curve in terms of  $[S_0, \Delta S]$  is continuous. However, the normalized entropy path of the grading curve in terms of  $[A, B]$  is not continuous. Some formulae can be derived for the discontinuity. If some  $i$  zero fractions are added from the smaller side (Fig 6).

$$B(N) - B(N + i) = \Delta S(N) \frac{1 - \frac{\ln N}{\ln N + i}}{\ln N} \tag{13}$$

The  $A$  change for  $i = 1, 2, \dots$  additional smaller zero fractions, respectively :

$$A(N + i) - A(N) = \frac{i[1 - A(N)]}{N + i - 1} \tag{14}$$

**Table 2.** The  $A$  coordinates for the fixed fractal dimension  $n = 2$  ( $a = 2$ , maximum  $S$  point), in the function of  $N$

$N$ [-]	2	3	4	5	6	7
$A$ [-]	0,667	0,714	0,756	0,790	0,819	0,843



**Figure 1** Simplex with  $N = 7$  (a) Lattice of continuous sub-simplexes (integers: fractions). (b) The image of the the optimal lines of continuous sub-simplexes in the non-normalised entropy diagram. (Az  $N = 7$  szimplex (a) a folytonos, határoló rész-szimplexeinek struktúrája, (b) optimális vonalak

képe a nem-normalizált entrópia diagramban.)

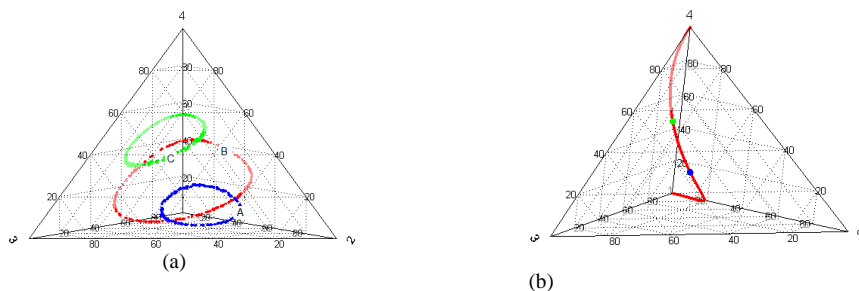


**Figure 2.** Simplex for  $N=4$ , the inverse image in the simplex for (a) three inner entropy diagram points (green  $A=0.66$   $B=1.2$ , red:  $A=0.5$   $B=1.2$ , blue:  $A=0.3$   $B=1.2$ ). (b) the maximum  $B$  line, called optimal line (in red). ( $N=4$ , 3-dimenziós szimplex. Az entrópia leképezés inverz képe a 3 dimenziós szimplexen. (b) Optimális vonal (b) Inverz kép (fentről lefele első:  $A=0.7$   $B=1.2$ , második:  $A=0.5$   $B=1.2$ , harmadik:  $A=0.3$   $B=1.2$ )).

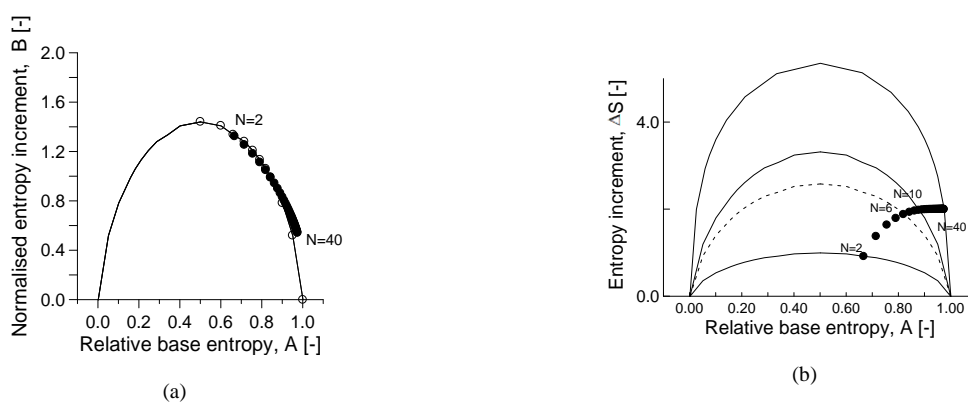


**Figure 3.** The image of the optimal points with the global maximum of  $S$  from  $N=2$  to  $N=40$  in (a) normalised diagram, (b) partly normalised diagram.

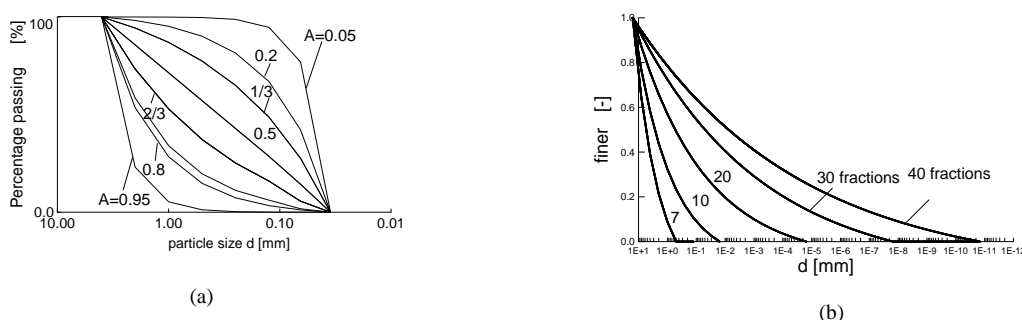


**Figure 4.** The optimal grading curves (a)  $N=7$ ,  $A$  varies. (b)  $N$  varies,  $A=2/3$ . (Optimális szemeloszlások, (a)  $N=7$ ,  $A$  változik, (b)  $N$  változik,  $A=2/3$ .)

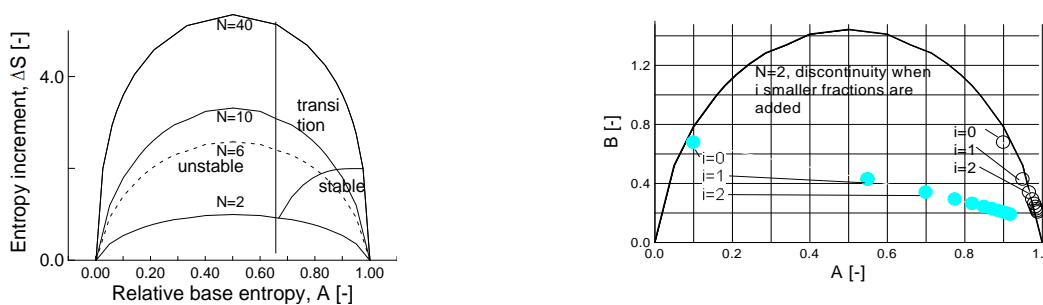


**Figure 5.** Internal stability criterion of Lőrincz (1986) in the partly normalized diagram. (Lőrincz (1986) belső stabilitási kritériuma a félig

**Figure 6.** Discontinuity of the normalized entropy path, in case of  $i$  new, smaller  $i$  (initially  $N=2$  optimal soil). (Számított szakadás a normalizált pályán, ha  $i$  db zérus nagyságú frakciót adunk a keverékhez a kisebb ol-

normalizált diagramon).

dalról,  $N=2$ , kezdetben optimális eloszlás esetén.)

### 3 EXPERIMENTS

#### 3.1 Crushing tests at the BME with topology change

The following testing procedure was developed. Each sample was subjected to a series of crushing treatments using a specially reinforced crushing device made at the Geotechnical Department with the following dimensions: diameter: 50 mm; height: 70 mm; wall thickness: 3 mm. Each treatment involved the application of a compressive load of 25,000 N to the sample contained in the crushing pot, using a loading machine at the Department of Construction Materials and Engineering Geology, BME. After the compression of the sample, it was removed from the crushing pot for grading curve measurement then was returned back and the treatment was repeated (Fig. 7, Lőrincz et al. 2005, 2017).

The results with a one-fraction soil is shown in Fig. 8. The results with initially 2-fraction silica and carbonate sands from the same initial grading and testing conditions are shown in Figs 9 to 10. These indicated the same entropy paths, only the rate of crushing was different. The non-normalised entropy path was monotonic ( $S_0$  decreased,  $\Delta S$  increased). The normalized path showed a jump when the number of the fractions was changing, at the start of the test. The discontinuity at the beginning of the test drifted the path into the stable region of the diagram. After the jump, a linear part of the entropy path occurred within the diagram ( $A$  decreased,  $B$  increased) until the maximum entropy increment line was reached. After reaching the maximum entropy increment line, the path followed it. The computed jump is in solid line in Figure 10 and the subsequent straight line path in dashed line.



**Figure 7.** Reinforced crushing pot designed by Lőrincz, used for crushing tests. (A Lőrincz által tervezett mini-mozsár)

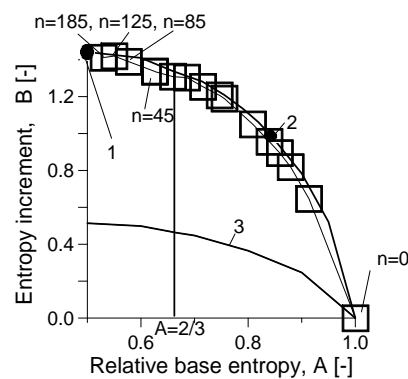
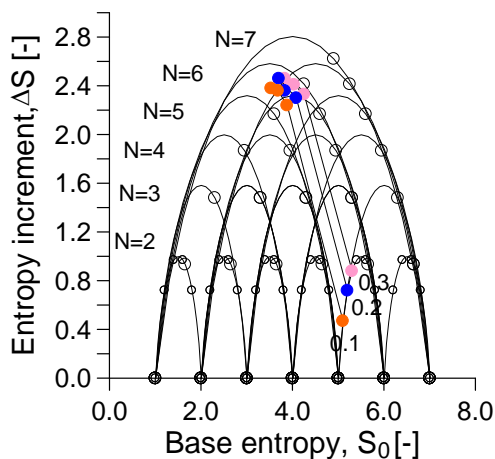
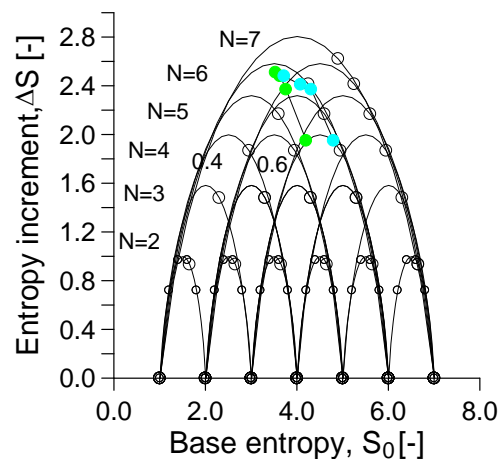


**Figure 8.** Normalised entropy path of a one-fraction soil.  $n$ : serial number of the crushing. 1: maximum B point. 2: maximum S point. 3: approximate minimum B line. (Normalizált entrópia pálya frakció esetén.  $n$ : törés-szám, 1,2: maximum B és S pont. 3: közelítő minimum B vonal.)



(\*a)



(b)

**Figure 9.** Non-normalized entropy path for initially  $N = 2$  soils, crushing test with topology change and with 30 crushing treatments. (a) carbonate soils, change in  $S_0 \sim 0,6$ ; change in  $\Delta S \sim 0,7$ . (b) Silica soils change in  $S_0 \sim 1,5$ ; change in  $\Delta S \sim 1,8$ . (*A nem-normalizált entrópia pályák. (a) mészkő homok (b) szilícium homok.*)

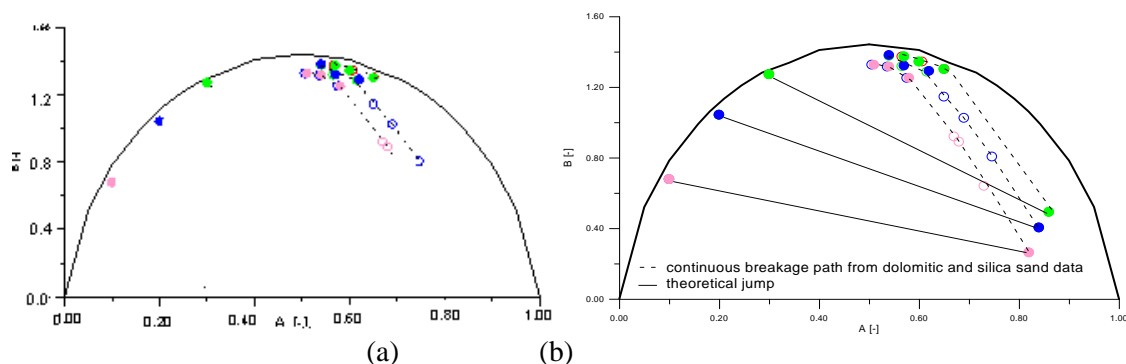


**Figure 10.** The normalised entropy paths of soils in Fig. 9. (a) Open circles indicate silica sand, full circles carbonate sand. (b) The computed jump in solid line and the subsequent straight part in dashed line. (*A normalizált entrópia pályák a 9. ábra talajaira. (a) Kör: szilícium homok, kitöltött kör: mészkő homok. (b) A számított szakadás (folytonos vonal) és az ezt követő egyenes szakasz (szaggatott).*)

### 3.1 Crushing tests at University of Roma Tor Vergata with topology change

The mechanical behaviour of granular materials with crushable grains under one-dimensional compression at medium to high stress has been tested by Casini *et al* (2013), the maximum load of tests reported by the authors is 2 MPa. The material used for the experimental work is a Light Expanded Clay Aggregate (LECA) whose grains break at relatively low stress (Casini *et al* 2013). Reconstituted samples were prepared with different initial grain size distributions and their evolution observed under one-dimensional compression (Casini *et al* 2017). In the frame of an ongoing research collaboration, some tests with large (50 MPa) load were made as follows. The oedometer cylinder ( $d=25\text{mm}$ ,  $h=42.5\text{mm}$ ) was filled through dry pluviation. Performing of the compression test till 50MPa with a displacement rate of 1mm/min, sieving was made and the post test material was treated again. The grain size distributions were reevaluated by fitting Weibull distribution (Guida *et al* 2016) assuming  $N=17$ , the results shown in Figure 11 are again similar to Figure 10.

## 4 DISCUSSION

### 4.1 Reanalysis of some laboratory tests with no topology change

Twenty five direct shear tests were conducted on dry granular rock fill material with particle sizes ranging from 19mm to 4.75mm. Two rock types were tested, a weak rock (Siltstone) and a strong rock (Andesite). The particle distribution of each test sample was determined prior and after testing. Two tests were carried out at each confining stress; a compression only test and a compression and shear test (Fityus and Imre' 2017, 2017a). The grain size distributions data are reevaluated on Figure 12 showing similar pattern as in the case of Figure 10.

### 4.1 Reanalysis of degradation path measured in open pit mine

The extraction of coal using open pit techniques disturbs vast areas of the land. The samples represented here came from sedimentary rock waste dumps of an open pit coal mine in the Hunter Valley of Australia, which the owners had been rehabilitating progressively. The soil particles are influenced by natural degradation due to eg., meteorological effects and fragmentation due to mechanical effects.

The samples were obtained by digging, taking care to avoid excessive particle breakage. Separate samples were taken from both the upper 150mm (the "topsoil"), and from the soil between 150 and 300mm deep (the "subsoil"). In the laboratory, the collected samples were oven dried and gently

sieved down to 150 microns using standard procedures. The material passing 150 microns was then analysed using a Malvern laser diffraction particle sizer, down to a fine particle size of 0.5 microns.

The relative base entropy  $A$  decreased, the entropy increment  $\Delta S$  monotonically increased during degradation. The largest fraction disappeared at the topsoil due to the meteorological degradation effects. The sample point pairs ( $N=17$ ) in the entropy diagram were situated close to the maximum normalised entropy increment line, having near-finite fractal distribution with fractal dimensions between 2.5 and 2.8 (computed using the “ $a$ ” parameter of the closest optimal mixtures with the same  $A$  values), according to expectation since the starting, undisturbed soil has fractal distribution (Fig. 13)

#### 4.1 The entropy path of crushing and degradation

The entropy path during crushing tests (or natural degradation or fragmentation) is monotonic for the non-normalised coordinates, the base entropy  $S_o$  decreases, the entropy increment  $\Delta S$  strictly monotonically increases. These reflect the decrease in mean diameter and the increase in the true entropy of thermodynamics (entropy principle).

The normalized path showed an initial jump when the number of the fractions was changing, at the start of the laboratory test (Figs 10 to 12), verifying the jump formulae (Eqs (17, 18)). After the jump, it was monotonic ( $A$  decreased,  $B$  increased), differing by a constant from the non-normalised coordinates. More precisely, a linear part may have occurred within the diagram until the maximum entropy increment line was reached then it was followed.

On the normalized entropy increment  $B$  line all distributions are fractal. The final point of the normalised path is possibly the global maximum of the normalised line. This diagram point is the symmetry point of upper bounding line of the normalized entropy diagram with fractal dimension 3, independently of the number of fractions  $N$ . For large  $N$  the  $n$  is close to 3 over a wide range of  $A$ .

In the laboratory crushing tests, the minimum grain size is limited by a crushing limit being around some microns Kendall (1978)). The largest fraction is not vanishing due to the ‘cushioning effect’ (Miao and Airey (2013)). Therefore, it can be assumed that after the start of the test, the number of the fractions is constant ( $N= N_{\max}$ ), and the final point of the non-normalised path is possibly the global maximum of the non-normalised line related to  $N= N_{\max}$ .

#### 4.1 A possible crushing rate definition

Since the path during crushing tests is monotonic in terms for the non-normalised coordinates, the base entropy  $S_o$  decrease or its normalised version during a given, fixed mechanical impact can be used for rock characterization with a nice physical meaning, reflecting the decrease in the mean diameter (defined properly by the grading entropy theory first, some results are shown in Fig 9, Table 3).

If the rate of the breakage is measured along the normalised entropy path, then a reference point and a size of the crushing treatment are necessary to be selected on the monotonic part of the path. The one fraction soils show monotonic normalized entropy path along the maximum  $B$  line (from  $A=1$ , Lőrincz et al, 2005, Fig 8). For an initially multi-fraction soil, there is a jump which be computed on the basis the suggested formulae, some computational results are shown in the Appendix and Table 3.

**Table 3.** Breakage rate characterization with the normalised and non-normalised mean diameter measure increments for an initially  $A=0.2$ ,  $N= 2$  soil, (see Figs. 9, 10, App.) (*A törési sebességet jellemző, átlagos szemcseátmérő mérőszám-változás azonos energiánál, 9-10. ábra és Melléklet*)

parent rock type	in $A$ [-], between 0-10 increment, monotonic part	in $S_o$ [-], between 0-30 increment
silica	<b>0,05</b>	<b>0,6</b>
carbonate	<b>0,18</b>	<b>1,5</b>

**Table 4.** Geometrical probability that an arbitrary grading with  $N$  fractions is stable. (A belső stabilitáshoz tartozó geometriai valószínűség különböző frakciószám esetén)

$N$ [-]	2	3	4	5	10	20	30
$P(A>2/3)$	3,33E-01	2,22E-01	1,67E-01	1,30E-01	4,16E-02	5,54E-03	8,24E-04

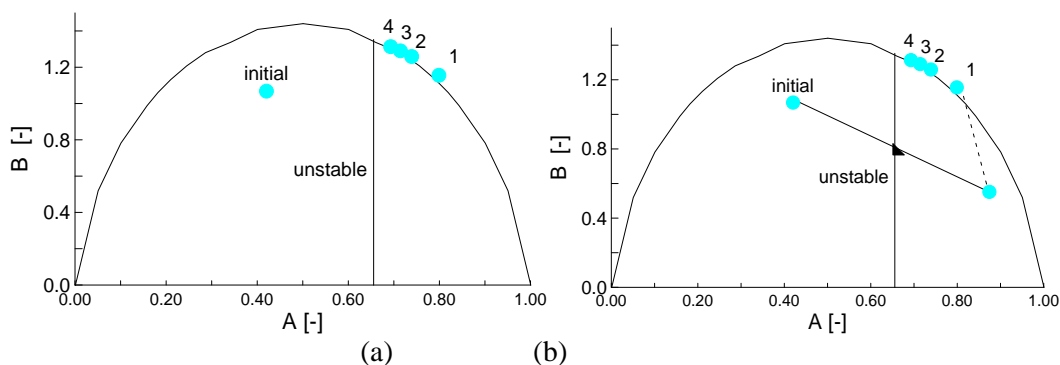


**Figure 11.** A soft rock multicompression test with topology change (Guida et al 2016; Casini et al 2017). (a) The normalised entropy path. (b) The computed jump in solid line and the subsequent straight part in dashed line. (*A normalizált entrópia pálya egy puha közet esetén. (a) Az eredmények. (b) A számított szakadás (folytonos vonal) és az ezt követő egyenes szakasz (szaggatott).*)

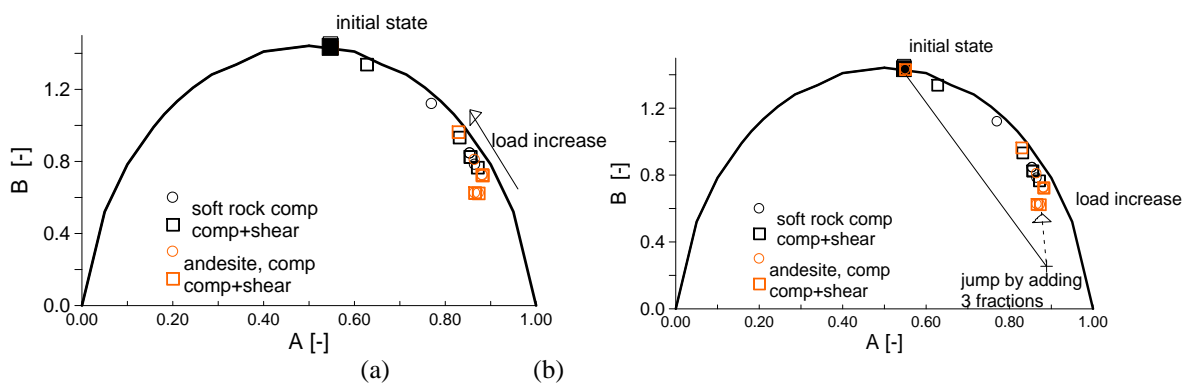


**Figure 12.** The compression-shear test data on andesite and soft rock. (a) The normalised entropy path. (b) The computed jump in solid line and the subsequent straight part in dashed line. (*Kompressziós-nyírási kísérletek, andeziten és puha közeten. (a) A normalizált entrópia pálya. (b) A számított szakadás (folytonos vonal) és az ezt követő egyenes szakasz (szaggatott).*)

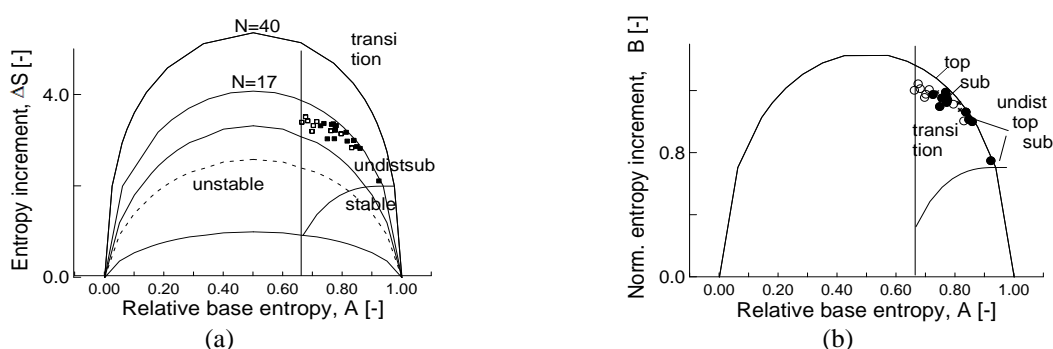


**Figure 13.** Degradation of waste rock in open pit mine rehabilitation, sample pairs of topsoil (open symbol, more degraded) and subsoil (full symbol, less degraded) in the (a) partly-normalized diagram and (b) in normalized diagram. (*Egy külszíni bányá meddő anyagának degradációja. A takaró és az alatta lévő alapréteg minta párok a (a) részben normalizált diagramon és a (b) normalizált diagramon, a takaró réteg (üres kör) jobban degradálódott, mint az altalaj (teli kör).*)

#### 4.1 Some comments on the degradation path and internal stability

As a result of breakage or degradation, the base entropy  $S_0$  decreases, the entropy increment  $\Delta S$  strictly monotonically increases. These express a decrease in the mean diameter (defined properly by the grading entropy theory first) and the entropy principle of thermodynamics. In the most general

case, the normalized entropy path may consist of 3 parts, the initial jump, a linear part which reaches the maximum entropy increment line then the path goes on the maximum entropy increment line upwards where all distributions are fractal. The final point of the path is possibly the global maximum of the normalized entropy increment  $B$  line.

The overall soil stability is described by the criterion that  $A > 2/3$ . In soils which meet this criterion, the matrix of coarser soil particles is stable and able to form a resistant skeleton, even though suffusion may occur. Concerning this rule, it is important to note that the size of the grading curve space where the condition is met is decreasing with the fraction number (e.g. for  $N=2$ , the 1/3 of the grading curves are acceptable, for  $N=3$ , the 2/9 of the grading curves are acceptable, for  $N=10$ , the 4/100 of the grading curves are acceptable, for  $N=30$ , the 8/10000 of the grading curves are acceptable, Table 9).

Concerning the maximum entropy increment line, the fractal dimension  $n$  varies between 3 and  $-\infty$  on the  $A > 0.5$  side,  $n$  varies between 3 and  $-\infty$  on the  $A < 0.5$  side of the maximum normalized entropy increment line. These depend on  $N$  except at the symmetry point of the diagram ( $A = 0.5$ ,  $B = 1/\ln 2$ ). At the symmetry point  $n = 3$ , independently of  $N$ . The distribution is unstable in terms of grading entropy criterion if  $A < 0.66$ . The related  $n$  depends on  $N$ , it is 2,62 for  $N=7$ , it is 2,25 for  $N=3$ , it is 2.96 for  $N=30$ . The fractal distribution is stable if  $n < 2$  (independently of  $N$ ,  $A$ ). Both the natural and the breakage data available – with fractal dimensions of around 2.2 to 2.96 – are generally related to the transitional stability zone on condition that the  $N$  is larger than about 5. This fact can be explained by the initial jump since without it the probability of an internally stable soils is practically zero for large  $N$  values. The jump is directly related to  $1 - A$ , being the larger if the initial  $A$  less. When some new, smaller fractions appear, the jump drifts the path to the  $A > 0.5$  side, more stable part of the diagram where  $n < 3$ .

The breakage path and the internal stability of natural soils seem to be deeply linked. The discontinuity at the appearance of some finer fractions may drift the normalised entropy increment path into the stable part of the diagram. In nature, stable fractal distributions occur due to the large degree of fragmentation and degradation, however, without this process, the probability that an arbitrary grading with  $N > 10$  fractions is stable is practically zero.

## 5 CONCLUSION

### 5.1 *Some comments on the entropy parameters*

The grading entropy parameters are some kind of integrals of the whole grading curve. These statistically are well-defined parameters and have some physical contents, as follows. The base entropy  $S_0$  is a weighed mean of the fraction serial number which depends linearly on the mean  $\log_2$  diameter  $d$ . The relative base entropy parameter  $A$  has a potential to be a grain structure stability measure possibly based on the simple physical fact that it expresses the ration of the larger grains and, if enough large grains are present in a mixture then these will form a skeleton. The entropy increment  $\Delta S$  measures how much the soil behavior is really influenced by all of its  $N$  fractions. For those grading curves, in which all  $N$  fraction s are well represented, the entropy increment is close to  $\ln N / \ln 2$ .

### 5.1 *Laboratory test for crushing rate characterization*

Since starting from the same normalized initial grading, the entropy path seems to be independent of the type of rock, a new laboratory rock qualification test can be elaborated. The results with silica and carbonate sands, the results with siltstone and andesite from the same initial grading and testing conditions indicated the same normalized entropy path, only the rate of breakage was different. The first results concerning the characterization of rate of crushing are as follows.

- The precise grading curve data are essential in computing the entropy path. If the fines are not measured, then the fitting of a proper eg., Weibull distribution (see eg., Guida at al (2016)) on the measured data is suggested. The number of fraction can be defined on the basis of the theoretical crushing limit.
- Starting from the same initial grading, the rate of the breakage can be defined in terms of the non-normalised or the normalised entropy path or both under the same mechanical energy input (see Table 3). The base entropy  $S_0$  reflects the decrease in the mean diameter. The normalized entropy path may consist of 3 parts, the initial jump, a linear part and a part along the maximum entropy increment line. A reference point is needed on the start of the monoton-

ic, continuous part of the path. Further research is suggested on the breakage rate definition and, on the comparison with standard rock tests.

## ACKNOWLEDGEMENT

This research work was initiated and supported by dr. Janos Lőrincz, his help is greatly acknowledged.

## References

- Airey, D W & Kelly, R B 2008. Interface behaviours from large diameter ring shear tests Proc of the res symp on the characterization and behaviour of interfaces, Atlanta, GA, USA, 1–6.
- Bridgwater, J., Utsumi, R., Zhang, Z. & Tuladhar, T. (2003). Particle attrition due to shearing – the effects of stress, strain and particle shape. *Chem. Engng Sci.* 58, No. 20, 4649–4665.
- Casini, F., Viggiani, G.M.B., Springman, S.M. 2013. Breakage of an artificial crushable material under loading. *Granular Matter* 15:661–673
- Casini F., Guida G., Bartoli M., Viggiani G.M.B. 2017. Grading evolution of an artificial granular material from medium to high stress under one-dimensional compression. *Rivista Italiana di Geotecnica*, 51(4): 69-80
- Coop, M. R., Sorensen, K. K., Bodas Freitas, K. K. & Georgoutsos, G. 2004. Particle breakage during shearing of a carbonate sand. *Geotechnique* 54(3): 157-163.
- Einav 2007. Breakage mechanics – Part I. Theory *Journal of the Mech. and Physics of Solids*, 55: 1274-1297.
- Fityus, S Imre, E 2017. The use of soil grading entropy as a measure of soil texture maturity JETC 2017. Poster presentation.
- Fityus S, Imre E 2017(a). The significance of relative density for particle damage in loaded and sheared gravels. *Powders and Grains 2017 – 8th International Conference on Micromechanics on Granular Media*, Montpellier, France, 03 Jul 2017 - 07 Jul 2017. Editors: Radjai F, Nezamabadi S, Luding S, Delenne JY . EPJ Web of Conferences. EDP Sciences, Les Ulis, France. 140: 4 pages. <https://doi.org/10.1051/epjconf/201714007011>
- Guida G., Bartoli M., Casini F., Viggiani G.M.B. 2016 - Weibull Distribution to Describe Grading Evolution of Materials with Crushable Grains. *Procedia Eng*, 158, pp. 75-80.
- Hagerty M M Hite D R Ulrich C R & Hagerty D J 1991 One-dimensional high-pressure compression of granular material *J Geotech Engng* 119 No 1 1–18
- Hartmann W K, 1969. Terrestrial, lunar, and interplanetary rock fragmentation. *Icarus* 10, No. 2, 201–213.
- Ho T Y K, Jardine R J & Anh-Minh N 2011 Large displacement interface shear between steel and granular media *Geotechnique* 61:3, 221–234.
- Imre B, Laue J, Springman S M. 2010. Fractal fragmentation of rocks within sturzstroms: insight derived from physical experiments within the ETH geotechnical drum centrifuge *Granular Matter* 12(3) 267–285.
- Imre E, Lőrincz J, Trang Q.P, Fityus S. Pusztai J, Telekes G, Schanz T. 2009 Some dry density transfer function for sands. Invited paper. *KSCE Journal of Civil Engineering* 13: (4) 257-272. 2009.
- Kendall, K. 1978. The impossibility of comminuting small particles by compression. *Nature* Vol 272. p. 710-711.
- Kun F, 2017. Breakage of particles, Session introduction. P&G Conference, Montpellier, 2017 July.
- Lőrincz J 1986 Grading entropy of soils Doctoral Thesis, Technical Sciences, TU of Budapest (in Hungarian).
- Lőrincz J, Imre E, Gálós M, Trang Q.P, Telekes G, Rajkai K, Fityus I. 2005 Grading entropy variation due to soil crushing. *Int. Journ. of Geomechanics*. Vol 5. Number 4. p. 311-320
- Lőrincz J, Imre E, Trang P Q, Fityus S, Casini F, Guida G. Grading entropy and breakage of Granular Matter. Manuscript, to appear in *Entropy*, JETC 2017. Theme Issue.
- Luzzani L, Coop M R 2002. On the relationship between particle breakage and the critical state of sands *Soils Found* 42(2) 71– 82
- McDowell G R, Bolton M D & Robertson D 1996. The fractal crushing of granular materials *J Mech Phys Solids* 44, No 12, 2079–2101.
- Miao, G. and Airey, D. 2013. Breakage and ultimate states for a carbonate sand. *Geotechnique* 63, No. 14, 1221–1229

- Okada Y Sassa K & Fukuoka H 2004 Excess pore pressure and grain crushing of sands by means of undrained and naturally drained ring-shear tests Engng Geol 75 No 3–4 325–343
- Pál G, Jánosi Z, Kun F and Main I G, 2016 Fragmentation and shear band formation by slow compression of brittle porous media, Physical Review E 94, 053003.
- Palmer A C & Sanderson T J O 1991 Fractal crushing of ice and brittle solids Proc R Soc London A Math Phys Sci 433. 1889. 469–477
- Roberts J E & de Souza J M 1958 The compressibility of sands Proc ASTM 58 1269–1277
- Sadrekarami A & Olson S M 2010 Particle damage observed in ring shear tests on sands Can Geotech J 47 No 5 497–515.
- Sammis C G, King G, Biegel R. 1987. The kinematics of gouge deformations Pure Appl Geophys 125, 777–812.
- Stacy S J & Sammis C G 1991 An automaton for fractal patterns of fragmentation Nature 353 250–252.

#### APPENDIX - RATE OF BREAKAGE FOR INITIALLY 2-FRACTION SOILS

Some numerical examples are presented for the initially 2-fraction soils shown 10, the jump point is considered as a reference point with zero treatment. The initial  $A$  value of the initially 2-fraction soils was 0.1, 0.2 and, the linear part of the path was used for the computation of the increments in entropy coordinates  $A$  and  $B$  for 10 crushing treatments.

The normalised entropy path, the jump was computed using Eqs (17) and (18), the related data in Tables A to C are denoted as 0 treatment. For this, it was assumed that the number of the fractions was increasing at the start of the test then it was constant. The increment in terms of  $A$  for silica or carbonate sand was around 0.05 or 0.19 between the point 0 and the point related to 10 treatments, resp. The increment in terms of  $B$  for silica or carbonate sand was around 0.36 or 0.9 between 0 and 10 treatments, resp. (The secant slope  $B/A$  between 0 and 10 treatments for silica sand was around -7, for carbonate sand was -4).

**Table A.** Normalised entropy path of silica and carbonate sands with identical initial ( $A = 0,2 N=2$ ) and jump coordinates (*Normalizált entrópia pálya azonos kezdeti ( $A = 0,2 N=2$ ) és szakadási pont esetén*).

rock type	Relative base entropy $A$ [-] at crushing no of					Normalized entropy increment $B$ [-] at crushing no of				
	initial	0 (jump)	10	20	30	start	0 (jump)	10	20	30
silica	0,2	0,8	0,746	0,69	0,65	1,04	0,44	0,805	1,02	1,14
carbonate	0,2	0,8	0,62	0,57	0,54	1,04	0,44	1,29	1,32	1,38
silica	0,1	0,77	0,73	0,68	0,67	0,68	0,27	0,639	0,88	0,919
carbonate	0,1	0,77	0,58	0,54	0,51	0,68	0,27	1,251	1,31	1,325

**Table B.** The 0-10 increment in terms of  $A$  and  $B$  related on the monotonic part of path to Table A. (Az első 10 törés alapján számított törési sebesség  $A$ -ban és  $B$ -ben kifejezve az A. táblázat adatai alapján).

$A = 0,2$	$A$ [-]	Increment in $A$ [-] at crushing treatments of				$B$ [-]	Increment in $B$ [-] at crushing treatment of			
rock type	initial	0 - initial	0-10	10-20	20-30	start	0 -start	0-10	10-20	20-30
silica	0,2	0,6	<b>0,05</b>	0,06	0,04	1,04	-0,59	<b>0,36</b>	-0,22	-0,12
carbonate	0,2	0,6	<b>0,18</b>	0,05	0,03	1,04	-0,59	<b>0,84</b>	-0,03	-0,06
silica	0,1	0,675	<b>0,05</b>	0,05	0,01	0,68	-0,40	<b>0,36</b>	-0,25	-0,03
carbonate	0,1	0,675	<b>0,2</b>	0,04	0,03	0,68	-0,40	<b>0,98</b>	-0,06	-0,01

**Table C.** Secant slopes on the monotonic part of path for Table B. (A szelő hajlása az B. táblázat adatai alapján).

$A = 0,2$	$A$	Increment in $B$ / Increment in $A$ at crushing treatment of		
rock type	initial	0-10	10-20	20-30
silica	0,2	<b>-6,60</b>	-3,91	-3,00
carbonate	0,2	<b>-4,67</b>	-0,60	-2,00
silica	0,1	<b>-8,08</b>	-5,00	-3,00
carbonate	0,1	<b>-5,00</b>	-1,60	-0,33